Received: 21 October 2022 | Revised: 7 June 2023 | Accepted: 7 June 2023

DOI: 10.1111/vru.13278

ORIGINAL RESEARCH

WILEY

Confirmed and presumed canine insulinomas and their presumed metastases are most conspicuous in the late arterial phase in a triple arterial phase CT protocol

Adrianna Skarbek | **Virginie Fouriez-Lablée** | **Helen Dirrig** | **Francisco Llabres-Diaz**

The Department of Small Animal Diagnostic Imaging, Queen Mother Hospital for Animals, Hawkshead Lane, Hertfordshire, Hatfield, United Kingdom

Correspondence
Adrianna Skarbek, The Department of Small Animal Diagnostic Imaging, Queen Mother Hospital for Animals, Hawkshead Lane, Hatfield, Hertfordshire, AL97TA, United Kingdom.
Email: askarbek21@rvc.ac.uk

Funding information
Royal Veterinary College—Transformative Agreement for Open Access

Abstract

Arterial enhancement is the commonly described characteristic of canine insulinomas in contrast-enhanced computed tomography (CECT). However, this finding is also reported as inconsistent. The main aim of this single-center retrospective observational study was to describe the contrast enhancement (CE) pattern of canine presumed and confirmed insulinomas and presumed metastases in three consecutive (early, mid, and late) arterial phases. Included dogs had a medical-record-based clinical or cytological/histopathological diagnosis of insulinoma and quadruple-phase CECT. The arterial phases were identified according to published literature. The arterial enhancement of confirmed and presumed lesions was assessed using a visual grading score. Twelve dogs with a total of 17 pancreatic nodules were analyzed. Three dogs had multiple pancreatic nodules and nine had solitary findings. Four insulinomas were histopathologically confirmed. Late arterial phase (LAP) images demonstrated the largest number of pancreatic nodules reaching the highest enhancement scores (n = 13, 76%). All analyzed dogs had CT evidence of arterially enhancing nodules in the liver (n = 12), seven in the hepatic, splenic, or colic lymph nodes, and three in the spleen. Three out of five sampled livers and three lymph nodes were metastatic. All sampled spleens were benign. Avid arterial enhancement was the most dominant feature of canine presumed and confirmed insulinomas and presumed metastases in quadruple-phase CECT. The highest enhancement scores were observed primarily in LAP, followed by MAP. Authors, therefore, recommend including LAP in the standard CT protocol for dogs with suspected pancreatic insulinomas.

KEYWORDS
CT angiography, enhancement, injection-duration, multiphasic CT

The authors followed STROBE reporting guidelines.

1 | INTRODUCTION

Diagnostic imaging findings, in combination with appropriate clinical signs and serum biochemistry, are often used to reach a presumptive diagnosis of insulinoma in dogs.[1–5] Multiple modalities are employed in the diagnosis of pancreatic tumors, including standard (US) and contrast-enhanced ultrasonography (CEUS), contrast-enhanced computed tomography (CECT), single-photon emission computed tomography (SPECT), scintigraphy and MRI.[6–8] CECT remains the most widely used technique for the detection of canine insulinomas, providing comparable results to human medicine.[9] Ultrasonography remains operator dependent and its sensitivity is low in diagnosing indistinct pancreatic nodules.[1,7] Scintigraphy and SPECT as single modalities are inferior to CECT and not commonly available.[7,8,10] MRI has shown good results in detecting canine insulinomas and their metastases but it is often less available in veterinary medicine than CECT.[6]

Preoperative detection and localization of pancreatic insulinomas are essential for surgical planning and successful resection of the tumor.[4,11] Exact localization of pancreatic nodules also affects the decision to perform open or laparoscopic surgery, which may become more available with current technical advances.[12,13] The laparoscopic access is determined by the location of the tumor which in turn dictates surgical positioning.[12] Pancreatic vascular supply is exclusively arterial, therefore late arterial and pancreatic phases have been reported to provide the best contrast between normal pancreas and parenchymal presumed lesions.[14,15] The scanning speed of multidetector CT (MDCT) scanners allows multiple arterial phases to be obtained after a single dose of contrast medium. In the early arterial phase (EAP), the contrast is not yet observed in the portal vein, whereas in the late arterial phase (LAP, also called portal inflow phase), initial enhancement of the portal vein and no or minimum hepatic parenchymal enhancement are present.[15–20] The difference between LAP and portal venous phase (PVP) is that in PVP the portal vein, portal tributaries, and the intrahepatic branches are fully enhanced, and the liver parenchyma demonstrates a peak of CE.[20] PVP is followed by the equilibrium phase when both portal and hepatic veins, and the liver parenchyma are homogenously enhanced.[20] The pancreatic phase represents the contrast phase, between arterial and portal phases when peak pancreatic enhancement occurs.[14,21,22]

CECT is widely used in many second opinion or referral veterinary centers and has shown good sensitivity in the detection of canine insulinomas.[9,10,12,23] Triple-phase CECT was proven superior to single- and double-phase CECT in tumor localization for presurgical staging.[12] Hyperattenuation in the arterial phase has been established as the most common CECT characteristic of human and canine insulinomas and their metastases.[15,17,18,23–25] However, more recent studies reported mixed results in the detection of arterially hyperattenuating insulinomas and their metastases in CECT.[7,9,10,12,15] Fukushima et al. and Buishand et al. reported only 22.2% and 47.1%, respectively, of arterially hyperattenuating insulinomas, whereas a later study documented predominance of tumor detection in the arterial phase.[9,10,12]

Considering the disparity in previous results, the aims of this study were (1) to investigate the arterial CE pattern of canine confirmed and presumed insulinomas and their presumed metastases in three consecutive arterial phases and (2) to determine whether one phase was more helpful than others. We hypothesized that there would be a difference in the conspicuity of pancreatic nodules and their presumed metastatic lesions depending on the arterial phase.

2 | MATERIALS AND METHODS

2.1 | Selection and description of subjects

This was a single-center retrospective clinical observational study. The initial inclusion criterium focused on dogs with quadruple-phase CT of the abdomen performed as described in detail below. The imaging database at Queen Mother Hospital for Animals of the Royal Veterinary College was searched for suitable cases between August 2018 and March 2022 using the DICOM "study description" tag with the institutional DICOM viewer (eUnity, Mach7 Technologies Canada Inc.) From all dogs with quadruple-CT images, the following criteria were used for inclusion in the study: medical records describing a clinical diagnosis of insulinoma, appropriate clinical signs (e.g., lethargy, weakness, seizures), appropriate biochemistry findings (persistent hypoglycemia and inappropriate hyperinsulinemia), appropriate imaging findings, and/or histopathology and/or cytology. Cases with quadruple-CT images and no clinical diagnosis of insulinoma were excluded. Institutional animal care and use approval was not obtained due to the retrospective study design. Decisions regarding patient inclusion or exclusion were reached by consensus by an ECVDI radiology resident (A.S.) and an ECVDI-certified veterinary radiologist (F.L.D.).

2.2 | Data recording and analysis

The signalment (age, sex, breed, body weight), clinical signs, biochemistry, appearance of insulinoma and metastases in the CT, cytological and histological results, and the time interval between imaging and sampling were recorded by the second year ECVDI resident (A.S.).

Pre- and postcontrast abdominal CT images of the abdomen of the included dogs were also reviewed by the radiology resident (A.S.) and the arterial phases were characterized as early, middle, and late arterial phases. Based on our review of the literature, this proposed classification had not been described for veterinary patients. Therefore, the following definitions were used in the current study (Figure 1A–D). In the EAP, solely the hepatic arteries were opacified. A partial opacification of the hepatic CVC with no or very faint contrast blush in the portal vein (PV) was considered as the middle arterial phase (MAP). The LAP was identified when clear inflow of contrast was observed in the PV at the porta hepatis with increased opacification of the CVC compared with MAP. All phases were characterized by marked enhancement of

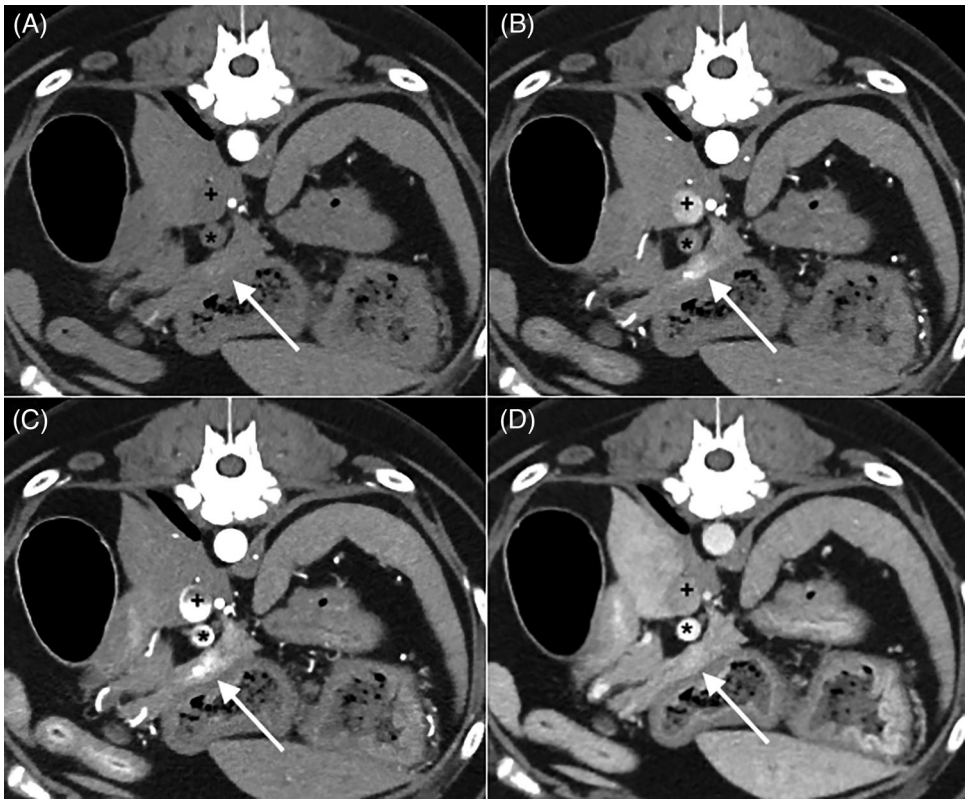

FIGURE 1 Transverse computed tomography images of a 10-year-old female neutered Labrador retriever illustrating; A, early (EAP); B, middle (MAP); C, late (LAP) arterial phases; D, venous phase. Progressive opacification of caudal vena cava (+) is noted. In LAP, the portal influx of contrast is observed in the portal vein (*). This is not observed in MAP. The arrow indicates progressive enhancement of the insulinoma graded as 0 in EAP, 2 in MAP, 3 in LAP, and 1 in venous phase. All images are displayed in soft tissue window (width: 400, level: 40), a slice thickness of 2.0 mm.

the abdominal aorta. Median time to threshold-aortic enhancement, interscan delays, median times to initiate each arterial phase, and median scan duration per arterial phase were retrospectively analyzed based on the bolus graphs generated for each CT study.

The CT studies were first reviewed during a single session by a radiology resident (A.S.) and an ECVDI-certified veterinary radiologist (F.L.D.), both of whom were aware of the clinical diagnosis. All cases were separately analyzed by another ECVDI-certified veterinary radiologist (V.F.L.), blinded to the previous observer assessments but not the clinical diagnosis of insulinoma. The final interpretation was reached by consensus of these three collaborators in a single session.

All assessments were performed with the same DICOM viewer (eUnity, Mach7 Technologies Canada Inc.) and a soft tissue window (window width: 400, window level: 40). Transverse images were evaluated for all cases, with adjustable multiplanar reconstructions, if necessary. The term " metastasis" was used to describe arterially enhancing foci identified in CT in organs other than the pancreas and which were consistent with previously reported imaging criteria for canine insulinoma metastasis.[9,17,25] For each pancreatic nodule or presumed metastatic lesion, the area with the highest enhancement was graded, regardless of the dimensions or degree of heterogeneity. The following data were recorded for each arterial phase: (1) presence and number of the arterially enhancing pancreatic nodules (each nodule was assessed individually); (2) visual grading score (VGS) of the CE of each pancreatic presumed lesion on a 4-point subjective grading scale (0, none/inconspicuous enhancement; 1, poor; 2, good; 3, excellent [the subjectively strongest aortic enhancement in EAP, MAP, or LAP was used as a reference for the "excellent" grade in the VGS]); (3) the location of the pancreatic nodules (body, right or left pancreatic lobes) and the agreement between CT and the surgical localization of pancreatic nodules; (4) presence, number and the same VGS of the arterially enhancing lymph nodes, hepatic, and splenic presumed lesions. If more than 50 avidly arterially enhancing hepatic nodules were identified, a >50 cut-off was recorded. In the spleen, only clearly defined arterially enhancing nodules were counted. The spleens with poorly-defined diffuse contrast distribution were excluded, as inhomogeneous contrast distribution may be normal in early phases.[15,16] HU values were not used for grading the CE of the presumed lesions since this study aimed to test the practical clinical application of each arterial phase for the detection of canine insulinomas and presumed metastases. The mean radiation doses of the quadruple-phase CTs were recorded and subjectively compared with the other routinely performed oncological (head, neck, thorax, and abdomen) and dynamic (temporal acquisitions) intravenous urography studies at the same institution. The effective doses (ED, mSv) were estimated based on dose length product (mGy*cm) and conversion factors (k-factors) for the abdomen adapted from human medicine, as described elsewhere.[26]

All data were entered into a spreadsheet (Excel for Mac, version 16.56, Microsoft) and initial descriptive analyses were performed by the radiology resident (A.S.). Additional descriptive statistics of the collected data were performed by the radiology resident (A.S.) and ECVDI-certified veterinary radiologist (F.L.D.) using commercially available software (SPSS IBM, New York, NY). The Mantel Haenszel Chi-square test was used to test the relationship between the arterial phase classification and VGS values.

3 | RESULTS

3.1 | Signalment

Twelve dogs were included in analyses. Breeds were as follows: crossbreed (n = 4), Labrador retriever (n = 2), French bulldog (n = 2), Yorkshire terrier (n = 1), Boxer (n = 1), Cocker spaniel (n = 1), Standard Poodle (n = 1). The median age was 10 years (range: 5–15) and the median body weight was 27 kg (range: 8–32.1 kg). The group consisted of neutered males (n = 6), neutered females (n = 5), and an intact male (n = 1). All the dogs presented with hypoglycemia, inappropriate hyperinsulinemia, abnormal mentation, lethargy, and weakness. Five dogs presented with seizures.

3.2 | Imaging techniques

The CT studies were performed under general anesthesia in three dogs and under sedation in nine. The standard sedation protocols consisted of intravenous administration of butorphanol (0.2–0.3 mg/kg, Dolorex 10 mg/mL, MSD Animal Health) and medetomidine (5 mcg/kg, Medetor 1 mg/mL, Virbac Limited). The anesthetic protocols varied between patients and consisted of premedication (methadone 0.1 mg/kg, Synthadon 10 mg/mL, Animalcare Limited; and/or midazolam 0.2 mg/kg, Hypnovel 10 mg/5 mL, Roche Products Ltd; and/or butorphanol 0.2 mg/kg, Dolorex 10 mg/mL, MSD Animal Health) and induction agents (alphaxalone 1 mg/kg, Alphaxalone Multidose 10 mg/mL, Jurox Animal Health; or propofol 1 mg/kg, PropoFlo Plus 10 mg/ml, Zoetis). The anesthesia was then maintained with a mixture of volatile anesthetic agents in oxygen. The CTs images were acquired in sternal recumbency with a 320-slice CT (Aquilion ONE-Genesis, Canon Medical Systems, Japan) before and after contrast (2 mL/kg; Omnipaque, 300 mg iodine/mL, GE Healthcare, UK) administration via the cephalic vein using a pressure injector (Medrad Stellant CT dual Injection System, Bayer Medical Care B.V., the Netherlands). The imaging protocol included three arterial and a venous phase (VP) with the following settings: 120 kVp, slice thickness 2–3 mm, 0.8–1.4 pitch, matrix size 512 × 512, a soft tissue/smooth reconstruction algorithm and image field-of-view tailored individually. The mAs was individually modulated, using ^{SURE}Exposure™ software (Canon Medical Systems, Otawara, Japan). A fixed injection duration (20 s)[27] and bolus tracking technique, triggered at 180 Hounsfield units (HU) in the region of interest (aorta at the diaphragmatic hiatus) were used. The contrast flow rates were adjusted according to the body weight based on previously described protocols.[27,28] The first images were obtained from cranial to caudal immediately followed by the second and third arterial phases obtained in caudal to cranial and cranial to caudal directions, respectively. A 60-s delayed (from contrast injection initiation) postcontrast phase was then acquired. The start and end locations for the arterial phases were the diaphragm and pelvic inlet/coxofemoral joints, respectively. The end location of the venous phase was set just caudal to the perineum.

3.3 | Description of pancreatic nodules and patient outcome

A detailed description of number, location, and means of diagnosis and sampling results for each patient is provided in Supporting information S1. A total of 17 pancreatic nodules were assessed. Nine dogs had solitary presumed lesions, two had three nodules each, and one dog had two pancreatic nodules. All nodules demonstrated arterial enhancement. The size, shape, and CT features of the pancreatic nodules were variable and described as rounded, ovoid, or irregular, well to poorly defined presumed lesions with heterogenous or homogenous arterial CE.

In eight dogs the diagnosis was established based on a combination of clinical signs, biochemistry, and CT findings. Four dogs of the total 12 dogs (three with solitary and one with two pancreatic nodules, total n = 5 pancreatic nodules) underwent partial pancreatectomy with histological confirmation of insulinomas. The distribution of the pancreatic nodules in CT varied, but the majority were identified in the body (n = 8), five in the right lobe and four in the left lobe of the pancreas. From four surgical cases, the CT localization of four nodules agreed with the surgical findings. In one of the dogs with a solitary nodule, CT localization was the pancreatic body but the tumor was found in the left lobe of the pancreas in surgery.

Eight out of 12 dogs (two with confirmed insulinomas and six with clinical diagnosis) improved after surgery and/or medical treatment initiation. One dog suffered a fatal cardiac arrest whilst recovering from general anesthesia after the CT scan. One dog underwent elective euthanasia postdiagnosis. Two dogs developed postsurgical complications (severe acute pancreatitis and aspiration pneumonia) and were euthanized 19 and 7 days after surgery, respectively.

3.4 | Cytological/histopathological results of the "metastatic" presumed lesions

Cytology and/or histopathology results of presumed metastases were available for five dogs (Supporting information S1). The ultrasound-guided sampling occurred immediately or within 2 days of the CT. One dog underwent surgery and biopsies two weeks after imaging. Two of four dogs that underwent surgery had surgical biopsies of the liver and identified abnormal regional lymph nodes. Histopathology of those samples revealed benign hepatic disease for both cases and metastatic

TABLE 1 Visual grading scores of insulinomas in consecutive contrast phases.

Visual grading score / Contrast phases	None/inconspicuous enhancement (grade 0)	Poor contrast enhancement (grade 1)	Good contrast enhancement (grade 2)	Excellent contrast enhancement (grade 3)
EAP	11 (65%)	6 (35%)	0	0
MAP	0	1 (6%)	15 (88%)	1 (6%)
LAP	0	0	4 (24%)	13 (76%)
Venous phase	10 (59%)	7 (41%)	0	0

Note: Number of pancreatic nodules (n = 17) in each grading category across the different contrast phases according to the applied visual grading score.
Abbreviations: EAP, early arterial phase; LAP, late arterial phase; MAP, middle arterial phase.

splenic and hepatic lymph nodes, respectively. Three dogs with clinical diagnosis of canine insulinomas had ultrasound-guided fine needle aspirations (FNAs) of the identified hepatic nodules. The cytology from all sampled hepatic presumed lesions revealed metastatic insulinomas. The cytology of the hepatic lymph node of one of those dogs also revealed metastatic insulinoma. The cytology (n = 1) and histopathology (n = 1) of the sampled splenic presumed lesions showed benign processes. The cytologically or histopathologically confirmed lesions mentioned above all demonstrated avid arterial enhancement.

3.5 | Visual grading score of the pancreatic and presumed metastatic lesions

The VGS values recorded for each of the pancreatic nodules in each arterial and venous phase are presented in Table 1. The largest number of non-/inconspicuously enhancing nodules was identified in EAP and the VP (65% and 59%, respectively). The largest number of nodules reaching excellent CE was achieved in LAP (76%). In MAP, most of the nodules (88%) scored good and only one (6%) reached excellent CE. In both MAP and LAP, none of the nodules were graded with none/inconspicuous enhancement. Conversely, none of the nodules reached good or excellent CE in EAP or VP.

Arterial contrast enhancement characteristics previously reported with metastasis[12] and interpreted as possible metastases for the current study were identified in 12 livers, 8 lymph nodes in 7 patients, and 3 spleens (Supporting information S1). CE of these presumed lesions was similar to the pancreatic nodules with the tendency of increasing enhancement toward LAP. In the liver, the presumed lesions presented as multiple-rounded, poor to well-defined, avidly contrast-enhancing nodules of variable sizes and locations in the hepatic parenchyma. Six dogs had fewer than 10 nodules, four between 10 and 20, and two dogs had more than 50 nodules. Eight arterially enhancing lymph nodes were recorded - three hepatic, three colic, and two splenic lymph nodes. The affected lymph nodes were described as mildly enlarged. The VGS of the hepatic presumed lesions and enhancing lymph nodes in each arterial and VP are presented in Table 2 (Figures 2A–D and 3A–D). None/inconspicuously enhancing hepatic presumed lesions and lymph nodes were identified only in EAP and VP. In those phases, none of the presumed lesions reached excellent CE. The largest number of hepatic presumed lesions and lymph nodes reaching excellent CE was achieved in LAP (59% and 50%, respectively). In MAP, most of the hepatic nodules and lymph nodes reached good CE (50% and 40%, respectively). In MAP and LAP, none of the presumed lesions were graded with none/inconspicuous enhancement.

The possible relationships between the arterial phases and the grading score in all three anatomical locations (pancreas, liver, and lymph nodes) were tested using the Mantel Haenszel Chi-square test. Despite the low numbers across the different possible phases/scores/anatomical locations, a significant statistical correlation ($P < 0.001$) was found for each location, indicating an association between the consecutive arterial phases and the grading score, with more "excellent" grades seen in late arterial phases on all three anatomical locations.

In three cases, well-defined arterially enhancing presumed lesions were identified as possible metastases in the spleen. Those presumed lesions were not seen in precontrast images and EAP In MAP, two spleens reached good enhancement whereas in the third dog, the presumed lesion was only poorly enhancing. The same proportions were found in LAP (two spleens with good and one with poor enhancement). In the venous phases, two spleens were graded as poor and one as none/inconspicuous CE.

3.6 | Timings of contrast phases

The median time to threshold-aortic-enhancement from the start of the injection was 23.5 s (range: 11.5–32 s). The median time delay from reaching the 180HU threshold to the first arterial acquisition was 3.75 s (range: 3–7 s) and the median interscan delay between phases was 5.5 s (range: 3.1–8.3 s). These are dictated by the machine's hardware and software-related factors with an option of manual adjustment. The median time to EAP, MAP, and LAP after initiation of contrast administration was 27 s (range: 14–36 s), 33 s (range: 23–44 s), and 39.5 s (range: 30–54 s), respectively. The median scan duration of each arterial phase was 2.5 s (range: 1.8—4 s).

In ten (83.3%) out of twelve dogs, the CT characteristics of the consecutive arterial phases corresponded with the proposed definitions. In two dogs (16.6%), the timings of the arterial phases did not correlate with the definitions. In one patient, the labeled VP corresponded with LAP. In the other dog, the labeled MAP was compatible with LAP and the LAP with PVP.

TABLE 2 Total number of presumed metastatic livers (n = 12) and lymph nodes (n = 8) in each grading category and across the multiple phases according to the applied visual grading score.

Number of cases in each grade / Contrast phases		None/inconspicuous enhancement (grade 0)	Poor contrast enhancement (grade 1)	Good contrast enhancement (grade 2)	Excellent contrast enhancement (grade 3)
EAP	Liver	9 (75%)	2 (17%)	1 (8%)	0
	Lymph nodes	4 (50%)	3 (38%)	1 (12%)	0
MAP	Liver	0	5 (42%)	6 (50%)	1 (8%)
	Lymph nodes	0	1 (12%)	4 (40%)	3 (38%)
LAP	Liver	0	1 (8%)	4 (33%)	7 (59%)
	Lymph nodes	0	1 (12%)	3 (38%)	4 (50%)
Venous phase	Liver	7 (59%)	4 (33%)	1 (8%)	0
	Lymph nodes	8 (100%)	0	0	0

Abbreviations: EAP, early arterial phase; LAP, late arterial phase; MAP, middle arterial phase.

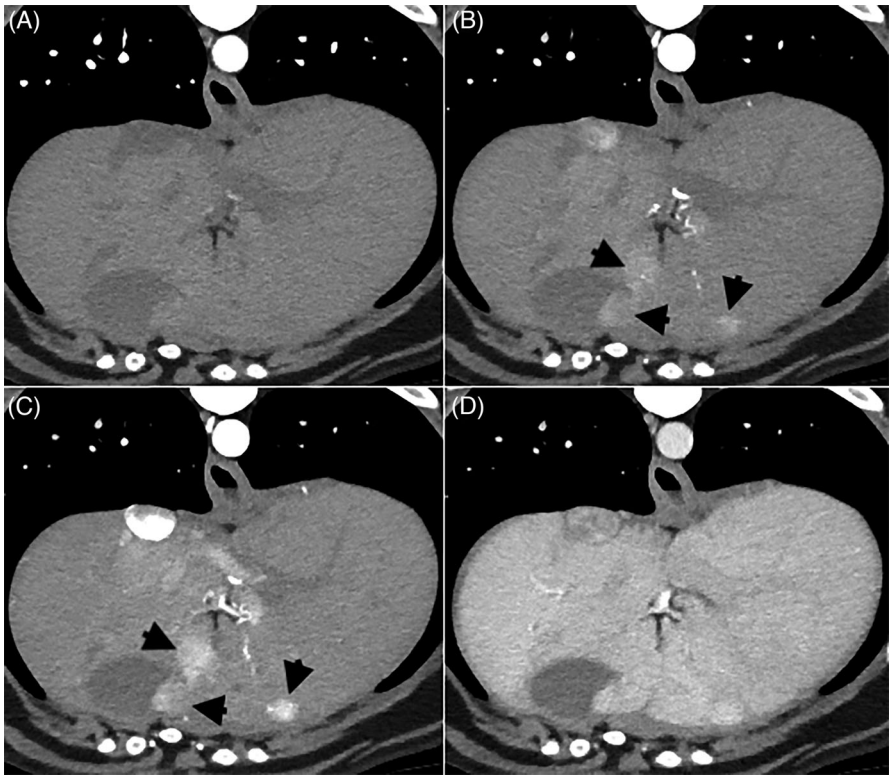

FIGURE 2 Transverse computed tomography images of a 10-year-old female neutered Labrador Retriever illustrating an example of the visual grading of cytologically confirmed hepatic metastatic lesions of insulinoma (arrowheads). A, grade 1 in EAP; B, grade 2 in MAP; C, grade 3 in LAP; D, grade 0 in the venous phase. All images are displayed in soft tissue window (width: 400, level: 40), slice thickness of 2.0 mm.

3.7 | Radiation dose

The estimated ED for the twelve patients (median: 30.9 mSv; range: 20.45–44.45 mSv) was lower than the estimated ED of dogs with a similar body weight that underwent dynamic intravenous urography (median: 54.38 mSv; range: 39.87–63.83 mSv) or a full body CT (head, neck, thorax, and abdomen) for the Oncology service (median: 39.94 mSv; range: 18.54–59.56 mSv).

4 | DISCUSSION

Based on our review of the literature, this is the first published study describing CE patterns of confirmed and presumed canine insulinomas in three consecutive arterial phases. All obtained images were of diagnostic quality and the scanning protocol allowed identification and separation of the described arterial and venous contrast phases. LAP provided excellent enhancement of the majority (76%)

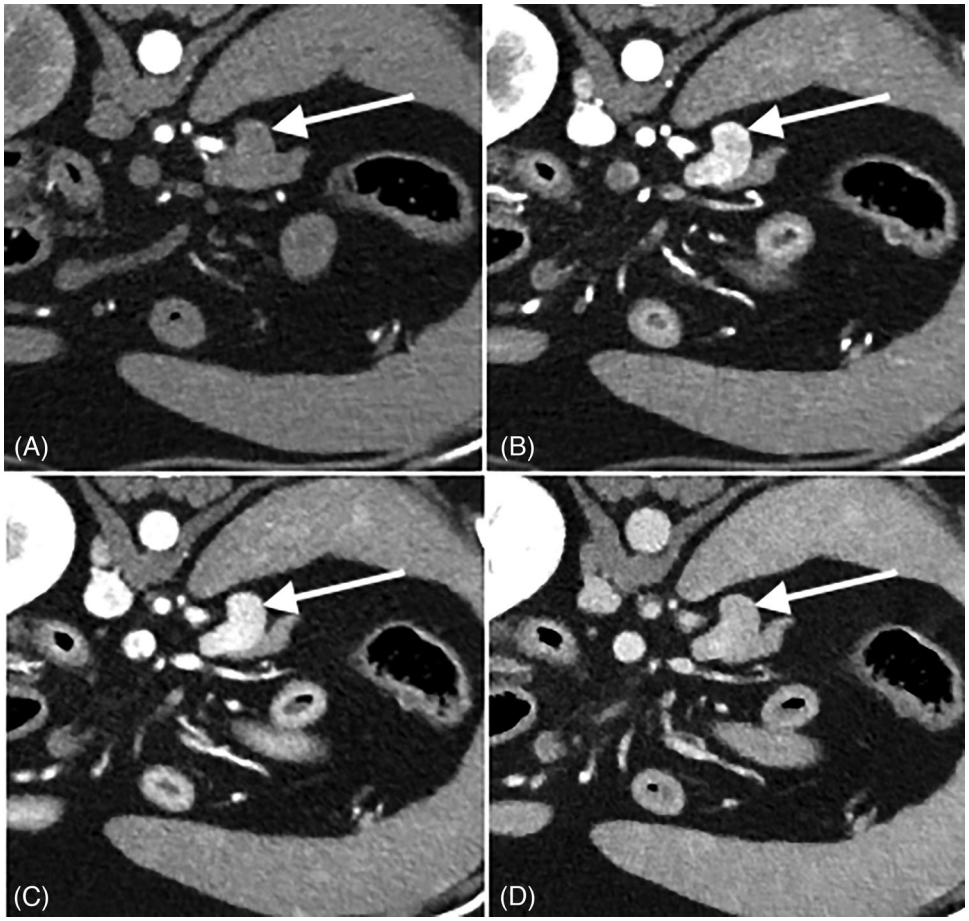

FIGURE 3 Transverse computed tomography images of a 10-year-old female neutered crossbreed dog illustrating an example of the visual grading of a histopathologically confirmed metastatic splenic lymph node (arrows). A, grade 0 in EAP; B, grade 2 in MAP; C, grade 3 in LAP; D, grade 0 in the venous phase. All images are displayed in soft tissue window (width: 400, level: 40), slice thickness of 2.0 mm.

of pancreatic nodules and presumed metastatic lesions. MAP was the second-best phase as nearly all insulinomas (88%) reached good CE, whereas the presumed nodules were mainly indistinct from the pancreatic parenchyma in EAP and VP and some of them might have gone unnoticed if not for the help of the concurrently displayed MAP and LAP. Moreover, a statistically significant relationship was found when testing the consecutive arterial phases and the higher enhancement score across the three different tested anatomical locations, with more excellent grades seen in late arterial phases. This agrees with our hypothesis that one of the phases would be superior at detecting the arterially enhancing presumed lesions. The results of this study also agree with the previously established arterial hyperattenuation of canine insulinomas as the most common CT feature.[24]

The lower incidence of arterial hyperattenuation described in previous studies could have resulted from various patient-, injection-, and scanning-related factors since different MDCTs, scanning, and contrast injection protocols were used. Unlike pancreatic adenocarcinomas, insulinomas are highly arterially vascular tumors, and therefore images acquired during arterial or pancreatic phases typically clearly demarcate the lesions.[17,24] Therefore, the progressive temporal arrival of contrast to the pancreas can explain the increasing enhancement of the presumed lesions toward excellent in LAP in 10/12 cases fitting the authors' definitions of EAP, MAP, and LAP.

The 320-row MDCT used in this study could routinely obtain three diagnostic arterial phases with minimal, if any, respiratory motion-related artifacts and supports the previous recommendation of selecting a fixed injection duration technique as a reproducible and less operator-dependent method of obtaining multiphasic post-contrast images with good vascular conspicuity. The description of three consecutive arterial phases is a novel addition to pancreatic imaging. We used a combined subjective assessment of the enhancement within the PV, CVC, and aorta at the level of porta hepatis to distinguish the phases. Portal influx of contrast in LAP has been previously described as a normal finding, likely due to equal distribution of contrast-enhanced blood within the aorta and cranial mesenteric vein during the arterial phase.[16,27] In veterinary and human literature the pancreatic phase falls between the arterial and portal phases[15] and is often defined by a 35–50 s scan delay, peak enhancement of the pancreatic parenchyma, and visible enhancement of the cranial mesenteric vein.[10,19,21,24] This phase is then followed by PVP, when the intrahepatic portal and hepatic veins are homogenously enhanced.[20] In our study, the median times to reach MAP and LAP after initiation

of contrast administration were 33 and 39.5 s, respectively, and therefore the pancreatic phase may overlap or be equal to LAP, as suggested in human medicine.[17–19] Additionally, the temporal window between LAP and the pancreatic phase may be too short and variable to successfully obtain both phases in a single study. The enhancement of the pancreatic parenchyma was not objectively quantified here, therefore more investigations are necessary to evaluate this further.

LAP may be more difficult to achieve in slower scanners or with different contrast injection methods as it typically immediately precedes PVP. In our case, the median arterial scan delay for EAP after time to aortic-threshold detection was 3.75 s, linked to table translation, but the acquisition was automatically triggered as soon as the bolus tracking threshold was reached. As a result of our study, at our institution, this interval to first arterial acquisition could be prolonged to 10–15 s for an insulinoma protocol when only LAP was sought. A similar variation could be tested with other scanners if the aortic threshold and the injection technique could be duplicated. Our results demonstrated that MAP (median 33 s after initiation of contrast administration) also provided adequate visualization of the pancreatic nodules in most of the patients. Practitioners with different MDCTs could therefore use those results as a guide to streamline their scanning protocols. A protocol could be devised so that, even with slower scanners, LAP (or MAP, depending on minimum scan delays between acquisitions) and a delayed VP could be obtained, bypassing PVP.

Patient-related factors, such as weight and cardiac output, are important to consider when undertaking CECT.[20,29] The temporal pattern of CE is influenced by cardiovascular circulation, with cardiac output being inversely correlated with arterial enhancement.[15,28] Both test-bolus and bolus tracking techniques are tailored to individual patients; however, the test-bolus method is still operator dependent and may not be ideal for fast scanners.[27] At our institution, the contrast injection time is fixed at 20 s and the flow rate is then tailored to body weight. Longer injection duration with lower injection rates can trigger a later and lower aortic peak enhancement; however, this did not decrease the quality of the images, regardless of the body weight, in previous reports and in our study.[27,28] Moreover, with a fixed-duration injection protocol, most of the acquired arterial phases (83.3%) corresponded with the definitions proposed by the authors. Only two dogs showed disparity between the labeled phases and the actual features of the acquired images. This possibly resulted from physiological patient-related factors. Previous reports describing CT features of canine insulinomas used fixed-flow rates and/or variable injection times, which could negatively influence the incidence of arterial hyperattenuating. In agreement with previous studies,[16,26,27] the authors recommend using a fixed injection duration time of 20 s to obtain wider bolus geometry and best vascular conspicuity in insulinoma CT protocols. In summary, the bolus tracking with fixed-injection-duration technique allowed consistent acquisition of all desired arterial phases providing arterial hyperattenuation of the insulinomas in all included dogs and would be the recommended injection technique to use when trying to apply the timings of the arterial phases from this study to other CT scanners.

Similar to primary tumors, insulinoma metastases to the liver, spleen, and local lymph nodes are also reported as hypervascular, and thus arterial phases presumably provide the best contrast between the lesions and the surrounding parenchyma.[25] Since 45%–55% of insulinoma cases have developed metastases at the time of presentation, identification of those lesions is an important prognostic factor.[1] Several studies described arterially enhancing lesions in the liver and regional lymph nodes in dogs with insulinomas.[9,10,12,23] Confirmed metastatic lesions in patients with insulinomas identified in MRI shared a similar appearance as the primary tumors.[6] Although less uniform, the enhancement pattern of the confirmed and presumed metastatic lesions in this study followed the tendency observed for insulinomas. Most of the presumed lesions could be identified both in LAP and MAP, showing good or excellent arterial enhancement. The latter was observed mainly in LAP. In EAP and VP, the hepatic presumed lesions were mainly non-/inconspicuously enhancing. A similar pattern was noted in the lymph nodes whereas in the VP all of them were already inconspicuous. Lymphadenomegaly without arterial enhancement was observed in two dogs. Due to absent arterial enhancement, these lymph nodes were not included in the descriptive part of the study; however, metastatic involvement cannot be excluded. Sampling of those lymph nodes was not performed. Definite diagnosis of metastasis requires cytological or histopathological confirmation. The CT appearance of confirmed malignant and benign lesions was impossible to distinguish based on imaging features alone. In humans, ultrasound-guided FNAs have been proven effective for the diagnosis of neuroendocrine tumors.[30,31] In our study, only hepatic cytology from FNAs confirmed insulinoma metastases whereas surgical biopsies diagnosed benign hepatopathies. This may have resulted from improved precision when targeting focal presumed lesions that may not be visible in surgery due to their deep location. Similar to FNAs, surgical biopsies represent only a fraction of a sampled organ, and lesions macroscopically indistinguishable from surrounding parenchyma during surgical assessment may remain unnoticed. In this study, none of the sampled spleens were found to be metastatic. Benign hypervascular hepatic and splenic lesions have been described.[32–34] Splenic extramedullary hematopoiesis, hepatomas, hepatic lymphoid, and nodular hyperplasia may present as arterially enhancing nodules or masses.[32–34] Benign hepatic lesions showed contrast retention during later CECT phases in a study.[33] This was not observed with identified confirmed and presumed metastasis included in this study. A recently published case series reported a sensitivity of 75% and 67% for the detection of hepatic and lymph node metastases, respectively.[12] In that study, only 8% of lymph nodes and 40% of livers with presumed metastases on the CT did not correspond with histopathological results. This is comparable with our study where the CT appearance of all sampled confirmed metastatic lymph nodes and 3/5 (60%) livers with confirmed metastatic lesions agreed with pathology results. Further investigations are necessary to better characterize metastases of canine insulinomas, considering both arterially enhancing and nonenhancing, abnormal organs.

Atypical insulinomas, which are iso- or hypoattenuating to the pancreatic parenchyma on contrast images, have been reported in human

medicine.[23,25,35] One report described a similar atypical appearance of a histopathologically confirmed insulinoma in CEUS and CECT where no CE was noted in any of the modalities.[36] This was not observed in our study, however, the lack of contrast enhancement in some insulinomas reported elsewhere means that the authors cannot exclude this possibility.[9,10] It is hoped that the careful evaluation of three consecutive arterial phases may have limited the possibility of lack of detection of presumed lesions enhancing at unusual timings. Further studies are required to investigate the occurrence and incidence of atypical canine insulinomas.

The main limitations of this study were the small sample size and its retrospective nature. All the images were initially reviewed in a single session by nonblinded observers; however, those results were later compared with the analysis of a third investigator, blinded to the previous grading. The investigators could assess all the arterial phases within a single window/hanging protocol, which could have influenced the identification of the poorly enhancing presumed lesions in EAP or VP. It is possible that fewer presumed lesions would have been detected in those phases if the observers were initially blinded to the results of MAP and LAP. The inter- and intra-observer agreements as well as the sensitivity and specificity of the subjective visual scores for the detection of presumed lesions were not statistically assessed, with an agreement regarding the CE scores reached by consensus. Further studies including objective assessment could be considered. Not all the identified presumed lesions had cytological or histopathological confirmations of insulinoma or its metastases. Although definite diagnosis can only be achieved by sampling, the provisional diagnosis, staging, and treatment of canine insulinoma relies chiefly on clinical data, serum insulin concentrations, and diagnostic imaging.[1] The scanning protocol described in this study and the scanning area were not standardized and differed slightly between patients. This may have affected the final presentation of time-to-aortic threshold and consecutive scan delays. The sedation or anesthetic protocols used were not analyzed in relation to patient-related factors affecting CE but all images were of diagnostic quality without detrimental effects of respiratory motion. Investigation of the influence of different anesthetic protocols and CE of canine insulinomas may warrant further studies. Additionally, due to the use of a fixed time 20 s injection protocol, the proposed definitions of contrast phases do not fully correspond to the generic angiographic definitions of arterial and venous phases linked to fixed injection rates protocols. Lastly, all dogs presented here were investigated with a 320-row MDCT scanner which is not widely available for veterinary use. The descriptions of the arterial phases were created retrospectively which may cause slight disparity if similar results are sought prospectively. Therefore, the results presented here should be tailored to each institution individually.

In conclusion, our study supported previous publications in that presumed and confirmed canine insulinomas and their metastases (presumed and confirmed) showed arterial hyperattenuation in CECT studies. In this study using a 320-slice MDCT, LAP followed by MAP subjectively improved the detection of the presumed lesions. The median time to reach MAP and LAP were 33 and 39.5 s after initiation of contrast administration, respectively, using a 20 s fixed injection duration protocol and the aortic threshold of 180 HU. The results presented here could guide the optimization of insulinoma protocols; however, the technical parameters should be considered before a change of protocol is made. The authors recommend the inclusion of LAP (and/or MAP) in the standard insulinoma protocol. Sole acquisition of early arterial and/or venous phases risks misdiagnosis due to very poor or absent CE of canine insulinomas and their presumed metastases.

AUTHOR CONTRIBUTIONS

Category 1

(a) Conception and design: Skarbek, Dirrig, Llabres-Diaz

(b) Acquisition of data: Skarbek, Fouriez-Lablée, Llabres-Diaz

(c) Analysis and interpretation of data: Skarbek, Fouriez-Lablée, Dirrig, Llabres-Diaz

Category 2

(a) Drafting the article: Skarbek, Fouriez-Lablée, Dirrig, Llabres-Diaz

(b) Revising article for intellectual content: Skarbek, Fouriez-Lablée, Dirrig, Llabres-Diaz

Category 3

(a) Final approval of the completed article: Skarbek, Fouriez-Lablée, Dirrig, Llabres-Diaz

Category 4

(a) Agreement to be accountable for all aspects of the work in ensuring that questions related to the accuracy or integrity of any part of the work are appropriately investigated and resolved: Skarbek, Fouriez-Lablée, Dirrig, Llabres-Diaz

CONFLICT OF INTEREST STATEMENT

The authors declare no conflicts of interest.

DATA AVAILABILITY STATEMENT

The data that support the findings of this study are available as supplementary files and from the corresponding author upon reasonable request.

PREVIOUS PRESENTATIONS

This research for accepted for oral presentation at the EVDI Annual Scientific Conference in Edinburgh in September 2023.

ORCID

Adrianna Skarbek https://orcid.org/0000-0002-4026-0064
Virginie Fouriez-Lablée https://orcid.org/0000-0003-4755-0977
Francisco Llabres-Diaz https://orcid.org/0000-0003-3966-1642

REFERENCES

1. Goutal CM, Brugmann BL, Ryan KA. Insulinoma in dogs: A review. *J Am Anim Hosp Assoc*. 2012;48(3):151-163.
2. Leifer CE, Peterson ME, Matus RE. Insulin-secreting tumor: Diagnosis and medical and surgical management in 55 dogs. *J Am Vet Med Assoc*. 1986;188(1):60-64.
3. Tobin RL, Nelson RW, Lucroy MD, Wooldridge JD, Feldman EC. Outcome of surgical versus medical treatment of dogs with beta cell

neoplasia: 39 cases (1990-1997). *J Am Vet Med Assoc*. 1999;215(2):226-230.
4. Polton GA, White RN, Brearley MJ, Eastwood JM. Improved survival in a retrospective cohort of 28 dogs with insulinoma: paper. *J Small Anim Pract*. 2007;48(3):151-156.
5. Cleland NT, Morton J, Delisser PJ. Outcome after surgical management of canine insulinoma in 49 cases. *Vet Comp Oncol*. 2021;19(3):428-441.
6. Walczak R, Paek M, Uzzle M, Taylor J, Specchi S. Canine insulinomas appear hyperintense on MRI T2-weighted images and isointense on T1-weighted images. *Vet Radiol Ultrasound*. 2019;60(3):330-337. doi:10.1111/vru.12715
7. Robben JH, Pollak YWEA, Kirpensteijn J, et al. Comparison of Ultrasonography, Computed Tomography, and Single-Photon Emission Computed Tomography for the Detection and Localization of Canine Insulinoma. *J Vet Intern Med*. 2005;19(1):15-22.
8. Garden OA, Reubi JC, Dykes NL, Yeager AE, McDonough SP, Simpson KW. Somatostatin receptor imaging in vivo by planar scintigraphy facilitates the diagnosis of canine insulinomas. *J Vet Intern Med*. 2005;19(2):168-176.
9. Coss P, Gilman O, Warren-Smith C, Major AC. The appearance of canine insulinoma on dual phase computed tomographic angiography. *J Small Anim Pract*. 2021;62(7):540-546.
10. Fukushima K, Fujiwara R, Yamamoto K, et al. Characterization of triple-phase computed tomography in dogs with pancreatic insulinoma. *J Vet Med Sci*. 2016;77(12):1549-1553.
11. Cornell K. Chapter 97: Pancreas. *Veterinary Surgery. Small Animal*. 2nd ed. Elsevier Saunders; 2017;1659-1973.
12. Buishand FO, Grosso FRV, Kirpensteijn J, van Nimwegen SA. Utility of contrast-enhanced computed tomography in the evaluation of canine insulinoma location. *Vet Q*. 2018;38(1):53-62.
13. Mcclaran JK, Pavia P, Fischetti AJ, Donovan TA. Laparoscopic resection of a pancreatic b cell tumor in a dog. *J Am Anim Hosp Assoc*. 2017;53(6):338-345.
14. Boland G, Maiiey ME, Saez M, Fernandez-del-castillo C, Warshaw AL, Mueller PR. Pancreatic-Phase Versus Portal Vein-Phase Helical CT of the Pancreas: optimal Temporal Window for Evaluation of Pancreatic Adenocarcinoma. *AJR Am J Roentgenol*. 1999;172(3):605-608.
15. Bertolini G. In: Bertolini G, ed. *Body MDCT in Small Animals: Basic Principles, Technology, and Clinical Applications*. Springer International Publishing; 2017;
16. Earley NF, Hall JL, Brown H, Schwarz T. Early partial portal venous contrast enhancement in canine CT-Angiography. *Vet Radiol Ultrasound*. 2020;61(6):628-635.
17. Noone TC, Hosey J, Zeynep F, Semelka RC. Imaging and localization of islet-cell tumours of the pancreas on CT and MRI. *Best Pract Res Clin Endocrinol Metab*. 2005;19(2):195-211.
18. Tamm EP, Bhosale P, Lee JH, Rohren E. State-Of-The-Art Imaging of Pancreatic Neuroendocrine Tumors. *Surg Oncol Clin N Am*. 2016;25(2):375-400.
19. Fidler JL, Fletcher JG, Reading CC, et al. Preoperative detection of pancreatic insulinomas on multiphasic helical CT. *Am J Roentgenol*. 2003;181(3):775-780.
20. Angiograph BertoliniG, Anomalies Vascular. *Adv Small Anim Care*. 2020;1:49-74.
21. Almeida RR, Lo GC, Patino M, Bizzo B, Canellas R, Sahani DV. Advances in pancreatic ct imaging. *Am J Roentgenol*. 2018;211(1):52-66.
22. Sahni VA, Mortelé KJ. The bloody pancreas: mDCT and MRI features of hypervascular and hemorrhagic pancreatic conditions. *Am J Roentgenol*. 2009;192(4):923-935.
23. Mai W, Cáceres AV. Dual-phase computed tomographic angiography in three dogs with pancreatic insulinoma. *Vet Radiol Ultrasound*. 2008;49(2):141-148.
24. Iseri T, Yamada K, Chijiwa K, et al. Dynamic computed tomography of the pancreas in normal dogs and in a dog with pancreatic insulinoma. *Vet Radiol Ultrasound*. 2007;48(4):328-331.
25. Sheth S, Hruban RK, Fishman EK. Helical CT of islet cell tumors of the pancreas: typical and atypical manifestations. *Am J Roentgenol*. 2002;179(3):725-730.
26. AAPM (2007) The Measurement, Reporting and Management of Radiation Dose in CT: Report of the AAPM Task Group 23. Report No.96, American Association of Physicists in Medicine, New York.
27. Thierry F, Chau J, Makara M, et al. Vascular conspicuity differs among injection protocols and scanner types for canine multiphasic abdominal computed tomographic angiography. *Vet Radiol Ultrasound*. 2018;59(6):677-686.
28. Davé AC, Ober CP, Rendahl A. Factors influencing enhancement timing in a triple-phase abdominal CT angiography protocol in dogs. *Am J Vet Res*. 2022;83(7):ajvr.21.03.0031.
29. Kan J, Milne M. Aorta, liver, and portal vein CT contrast enhancement during the portal venous phase are positively associated with abdominal fat percentage in dogs. *Vet Radiol Ultrasound*. 2021;62(4):437-444. doi:10.1111/vru.12957
30. Unno J, Kanno A, Masamune A, et al. The usefulness of endoscopic ultrasound-guided fine-needle aspiration for the diagnosis of pancreatic neuroendocrine tumors based on the World Health Organization classification. *Scand J Gastroenterol*. 2014;49(11):1367-1374. doi:10.3109/00365521.2014.934909
31. Sugimoto M, Takagi T, Hikichi T, et al. Efficacy of endoscopic ultrasonography-guided fine needle aspiration for pancreatic neuroendocrine tumor grading. *World J Gastroenterol*. 2015;21(26):8118-8124. doi:10.3748/wjg.v21.i26.8118
32. Cordella A, Caldin M, Bertolini G. Splenic extramedullary hematopoiesis in dogs is frequently detected on multiphase multidetector-row CT as hypervascular nodules. *Vet Radiol Ultrasound*. 2020;61(5):512-518. doi:10.1111/vru.12872
33. Fukushima K, Kanemoto H, Ohno K, et al. Ct characteristics of primary hepatic mass lesions in dogs. *Vet Radiol Ultrasound*. 2012;53(3):252-257. doi:10.1111/j.1740-8261.2011.01917.x
34. Fife WD, Samii VF, Drost T, Mattoon JS, Hoshaw-Woodard S. Comparison between malignant and nonmalignant splenic masses in dogs using contrast-enhanced computed tomography. *Vet Radiol Ultrasound*. 2004;45(4):289-297.
35. Matondang S, Suwita BM, Budianto T, Krisnuhoni E. Atypical CT and MR imaging of insulinoma: a case report. *J Clin Transl Endocrinol Case Reports*. 2021;19:100075.
36. Reunanen V, Laitinen M. Contrast-enhanced ultrasonographic detection and dual-phase computed tomographic angiography in a 5-year-old boxer with pancreatic insulinoma —case report. *Open J Vet Med*. 2015;05(07):175-180.

SUPPORTING INFORMATION

Additional supporting information can be found online in the Supporting Information section at the end of this article.

How to cite this article: Skarbek A, Fouriez-Lablée V, Dirrig H, Llabres-Diaz F. Confirmed and presumed canine insulinomas and their presumed metastases are most conspicuous in the late arterial phase in a triple arterial phase CT protocol. *Vet Radiol Ultrasound*. 2023;64:834–843. https://doi.org/10.1111/vru.13278